Fracture Mechanics Analyses of the Slip-side Joggle Regions of Wing-Leading Edge Panels

Ivatury S. Raju
NASA Langley Research Center
Hampton, VA,

Norman F. Knight, Jr.
General Dynamics Information Technology
Chantilly, VA,

Kyongchan Song
ATK Space Division
Hampton, VA,

Dawn R. Phillips
NASA Marshall Space Flight Center
Huntsville, AL

Extended abstract for the 9th Youth Symposium on Experimental Solid Mechanics (YSESM)
July 7-10, 2010, Triste, Italy

The Space Shuttle Orbiter wing comprises of 22 leading edge panels on each side of the wing. These panels are part of the thermal protection system that protects the Orbiter wings from extreme heating that take place on the reentry in to the earth atmosphere. On some panels that experience extreme heating, liberation of silicon carbon (SiC) coating was observed on the slip side regions of the panels. Global structural and local fracture mechanics analyses were performed on these panels as a part of the root cause investigation of this coating liberation anomaly. The wing-leading-edge reinforced carbon-carbon (RCC) panels, Panel 9, T-seal 10, and Panel 10, are shown in Figure 1 and the progression of the stress analysis models is presented in Figure 2. The global structural analyses showed minimal interaction between adjacent panels and the T-seal that bridges the gap between the panels. A bounding uniform temperature is applied to a representative panel and the resulting stress distribution is examined. For this loading condition, the interlaminar normal stresses showed negligible variation in the chord direction and increased values in the vicinity of the slip-side joggle shoulder. As such, a representative span–wise slice on the panel can be taken and the cross section can be analyzed using plane strain analysis.

Extensive fracture mechanics studies for extreme thermal loading conditions were performed with subsurface defects. Plane strain fracture mechanics models were developed using the Panel 10 slip-side joggle configuration with discrete layers of SiC coating and RCC substrate materials (see Figure 3). The transverse craze cracks in the SiC coating layers were explicitly modeled including craze crack edge interaction (or surface friction) when the edges are in contact. Two types of defects, subsurface defects at the interface between the SiC/RCC substrate (interface defects) and defects within the RCC substrate (substrate defects), were considered. Various lengths of defects along the joggle and in the acreage were analyzed. Both entry heating and on-orbit cold conditions were used in the analyses. The objective of the fracture mechanics analyses is to determine the defect-driving force associated with different subsurface defects. The total defect-driving force and its components are characterized by the strain energy release rates, G-values, computed using the virtual crack-closure technique (VCCT). The total defect-driving force is compared to a critical value. If the defect-driving force is less than the critical value then the defect is stable. If, on the other hand, the defect-driving force is greater than or equal to the critical value, then the defect will grow in an unstable manner and fast fracture is predicted to occur. Representative fracture mechanics results for interface defects are presented in this paper.

To study the effects of the interface defect location along the joggle, the interface defect is moved to the different craze crack locations shown in Figure 3 (i.e., from Location 0 (Baseline-I) to Location +1, then Location +2, etc.). For lift-off and ascent bounding loading cases, the G_T/G_{Ic} values obtained for the Baseline-I model are essentially zero. These loading conditions are considered to be benign, and hence, no further analyses are performed for interface defects subjected to the lift-off and ascent loading conditions.

The interface defect locations are analyzed for the bounding on-orbit cold thermal loading condition. For this condition, the craze cracks open and no craze crack edge interaction occurs. The results are shown in Figure 4. The deformed configurations for each defect location are shown at the top of the figure. The G_T/G_{Ic} values for the left and right defect tips are plotted at the bottom of the figure as a function of the horizontal distance from Location 0. The G_T/G_{Ic} values for both the left and right defect tips at every location are nearly constant, with the highest value at the left tip of the defect at Location 0, $G_T/G_{Ic} = 1.6$. The G_T/G_{Ic} values for all of the defect tips are greater than unity. Therefore, this condition requires further examination. If G_T is Mode I-dominated, then the defect is unstable. However, the fracture response for the on-orbit cold condition is a Mode II-dominated response, and the ratio of G_{IIc}/G_{Ic} is about four. Hence, such an interface defect is predicted to be stable for the bounding on-orbit cold condition.

The interface defect locations are analyzed for the bounding entry loading condition. For this condition, the craze cracks close and craze crack edge interaction occurs. The results are shown in Figure 5. The deformed configurations for each defect location are shown at the top of the figure. The G_T/G_{Ic} values for the left and right defect tips are plotted at the bottom of the figure as a function of the horizontal distance from Location 0 for two values of the coefficient of

friction μ: μ=0 for perfectly smooth surfaces and μ=0.4 smooth surfaces. The G_T/G_{Ic} values for the right tips are much higher than the G_T/G_{Ic} values at the left tips, with the highest value at the right tip of the defect at Location 0, G_T/G_{Ic} = 2.0 for μ=0 and G_T/G_{Ic} = 0.81 for μ=0.4. If G_T is Mode I-dominated, then the defect is unstable when the craze crack edges are perfectly smooth. The G_T/G_{Ic} values are less than unity when the craze crack edges are smooth (friction is included), and hence, these defects are stable.

From the global three-dimensional analyses, it was concluded that the slip-side joggle region was the region of interest, that increased interlaminar stress levels developed in this region for entry conditions, and that a plane strain modeling approach of this region is applicable for bounding analyses. From the fracture mechanics analyses of the interface defects, it was concluded that interface defects have the potential of becoming unstable and may lead to liberation of a coating 'island' during entry. From the analyses of the substrate defects, substrate defects also appear to have the potential to become unstable depending on their location and length along the joggle. This paper summarizes features of the global stress and fracture mechanics analyses and discusses some salient results.

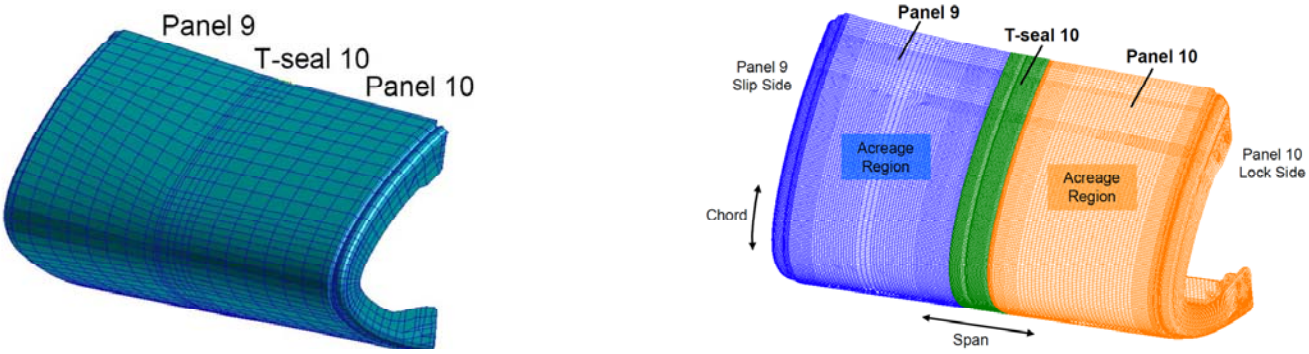

a) Global shell model (b) Global 3D model

Figure 1. Integrated model of Panel 9, T-seal 10 and Panel 10.

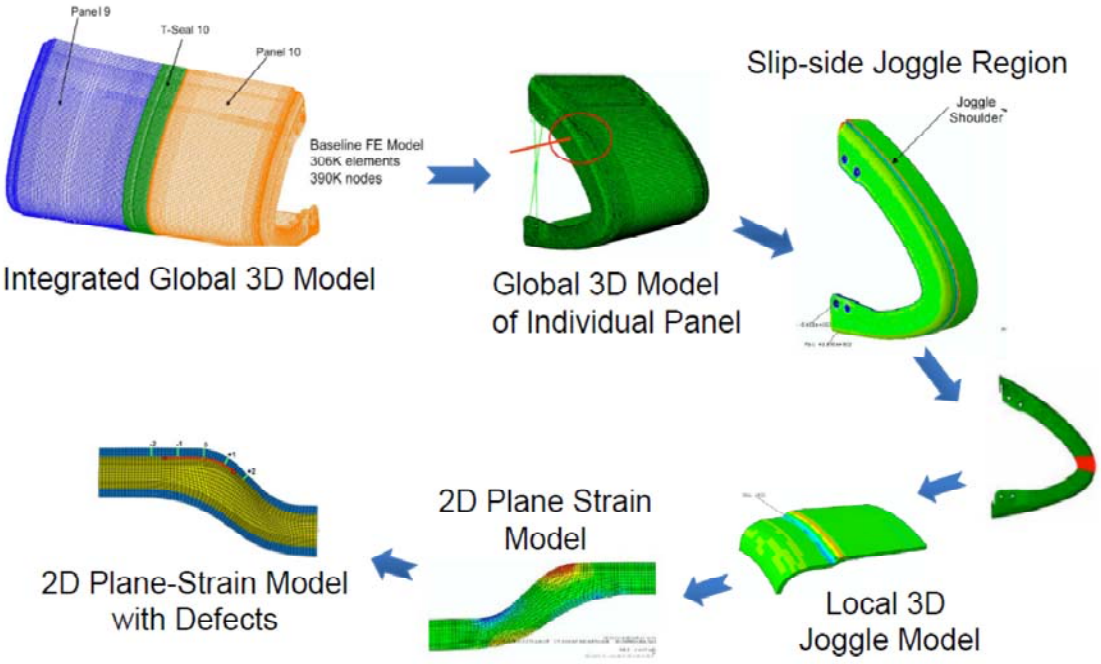

Figure 2. Global structural and fracture mechanics models.

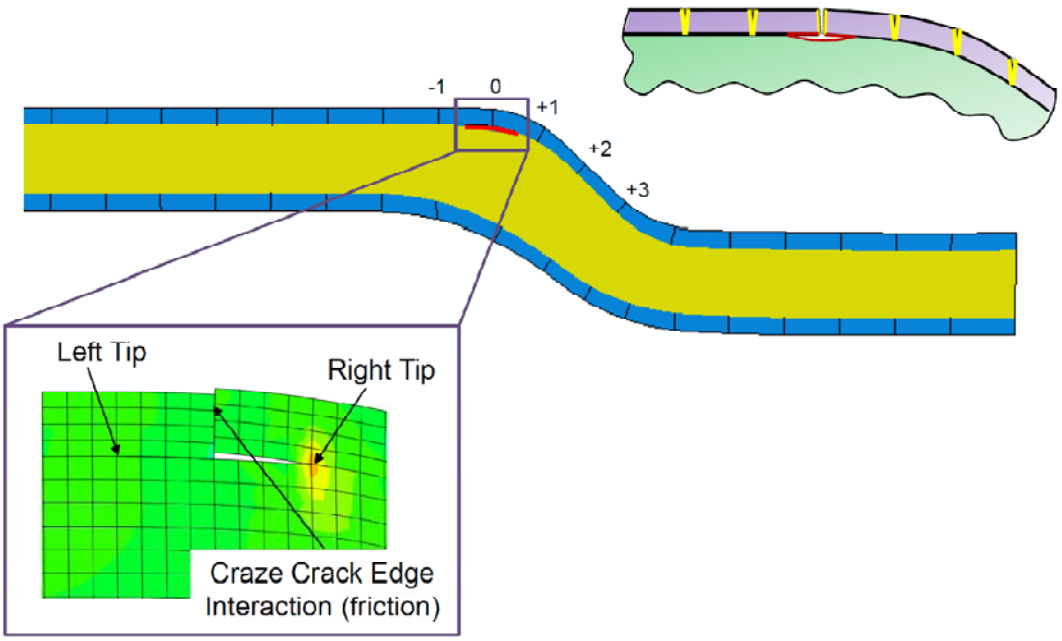

Figure 3. Slip-side joggle configuration with defect location index and Baseline-I interface defect at Location 0.

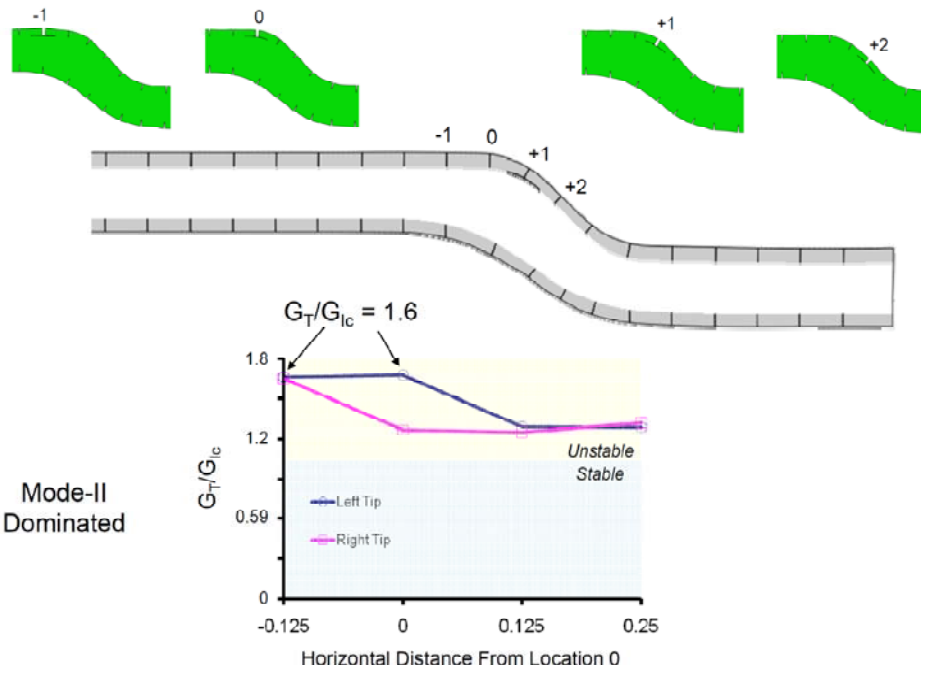

Figure 4. On-orbit deformed configurations and G_T/G_{Ic} values for single interface defect at different craze crack locations.

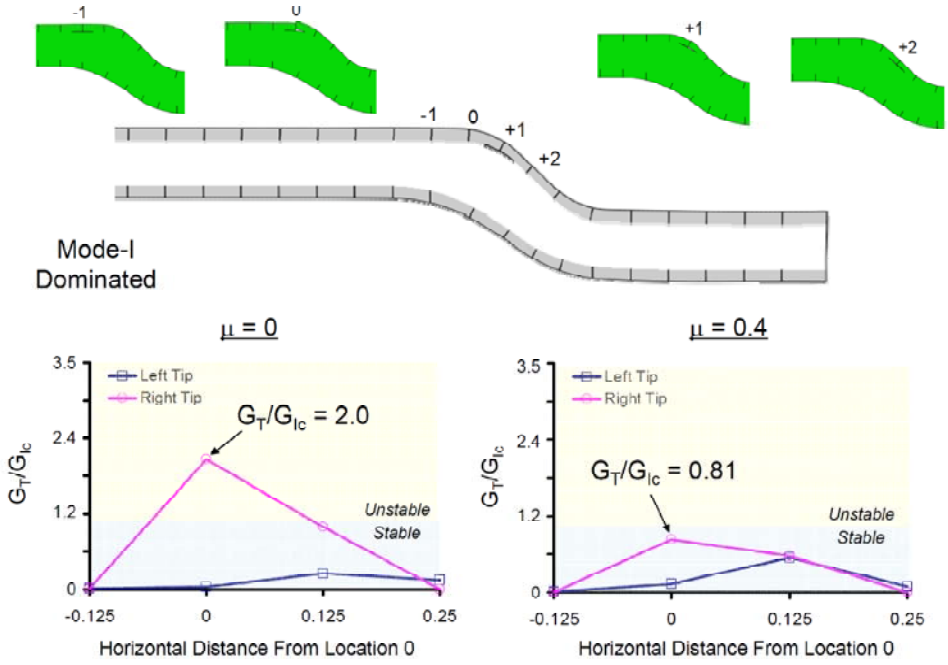

Figure 5. Entry deformed configurations and G_T/G_{Ic} values for single interface defect at different craze crack locations.